J-12

An Efficient Electromagnetic Analysis of Arbitrary Microstrip Circuits

James C. Rautio and Roger F. Harrington

Syracuse University
Syracuse, NY

ABSTRACT

A microstrip analysis suitable for monolithic microwave integrated circuits is described. The analysis subdivides microstrip metalization into small subsections and determines all currents and fields. Agreement between measured and calculated data demonstrates a high level of accuracy.

SUMMARY

A time-harmonic electromagnetic analysis has been developed for shielded microstrip circuits of arbitrary planar geometry. The analysis subdivides the microstrip metalization into small subsections and calculates the tangential electric field due to current on each subsection. The currents on all subsections are then adjusted so that the weighted residual of the total tangential electric field is zero on all metalization. The required currents form the solution and the N-port circuit parameters follow immediately.

The technique is a Galerkin implementation of the method of moments developed as an extension of an analysis of planar waveguide probes[1]. The technique expands the fields due to current in each subsection as a sum of rectangular waveguide modes. As such, it is closely related to the spectral domain approach [2] and is detailed in [3]-[7].

The analysis was implemented on an IBM-PC and later ported to a VAX 11/780. The IBM-PC version can analyze small circuits (10 or 20 subsections) in several minutes. Larger circuits (100 to 200 subsections) require several hours.

Several microstrip structures have been fabricated and measured. The circuits have dimensions on the order of centimeters to ease measurement requirements. Agreement between measured and calculated results suggests that in scaling the measured structure to the actual dimensions of a typical monolithic microwave integrated circuit, accuracy would be maintained to well above 50 to 100 GHz.

METHOD OF ANALYSIS

The microstrip circuit is contained in a rectangular conducting box treated as two separate waveguides joined at z=h (Figures 1 and 2) with the

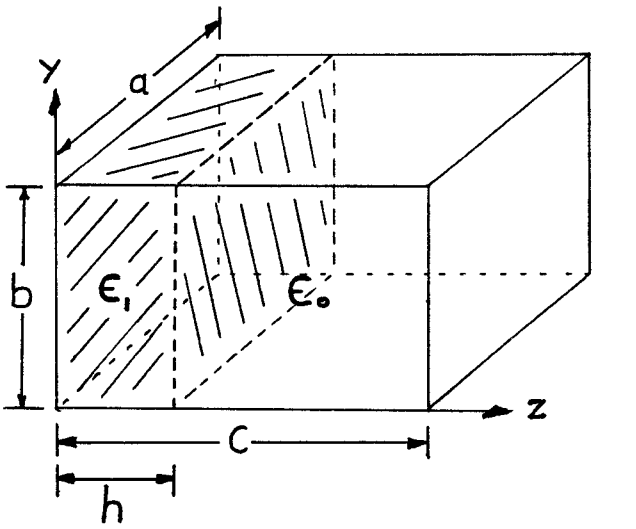

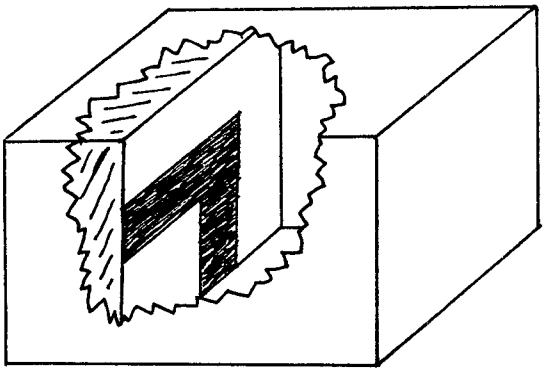

Figure 1. (top) Microstrip coordinate system.
Figure 2. (bottom) Example microstrip circuit.

indicated regions and dielectric constants. Note that region 0 is usually but not necessarily air.

The tangential (or transverse to z) fields in a given region due to current on a single subsection is expressed as a sum of homogeneous waveguide modes. Modes transverse to z are used with a z dependence such that the boundary conditions at z=0 for region 1 and at z=c for region 0 are met. Expressions for the tangential fields are written as a weighted sum of these modes

0149-645X/87/0000-0295$01.00 © 1987 IEEE

$$E_t^1 = \sum V_i \frac{\sin(K_{iz}^1 z)}{\sin(K_{iz}^1 h)} e_i$$

$$H_t^1 = \sum V_i Y_i^1 \frac{\cos(K_{iz}^1 z)}{\sin(K_{iz}^1 h)} h_i$$

$$E_t^o = \sum V_i \frac{\sin[K_{iz}^o (c-z)]}{\sin[K_{iz}^o (c-h)]} e_i$$

$$H_t^o = \sum V_i Y_i^o \frac{\cos[K_{iz}^o (c-z)]}{\sin[K_{iz}^o (c-h)]} h_i$$

where i = Summation index over all modes.

V_i = the modal coefficient of the i^{th} mode.

Y_i = the admittance of the i^{th} mode:

$$Y_i^{1TE} = jK_{iz}^1 / (\omega\mu_1), \quad Y_i^{1TM} = j\omega\epsilon_1 / K_{iz}^1$$

$$Y_i^{oTE} = -jK_{iz}^o / (\omega\mu_o), \quad Y_i^{oTM} = -j\omega\epsilon_o / K_{iz}^o$$

$$K_{iz}^1 = -\sqrt{K_1^2 - K_x^2 - K_y^2}, \quad K_{iz}^o = +\sqrt{K_o^2 - K_x^2 - K_y^2}$$

$$K_x = M\pi/a, \quad K_y = N\pi/b$$

$$K_1 = \omega\sqrt{\mu_1 \epsilon_1}, \quad K_o = \omega\sqrt{\mu_o \epsilon_o}$$

Note that the modal admittances are the admittances of the standing wave modes rather than those of the usual traveling wave modes (they differ by the constant j).

The e_i and h_i are the orthonormal mode vectors which form a basis for the expansion of the fields in each region. If a different geometry is selected for the waveguide shield, only the mode vectors need be changed.

Given a specific current distribution on the surface of the substrate, we must determine the modal coefficients, the V_i, of the field generated by that surface current. This is accomplished by setting the discontinuity in magnetic field equal to the assumed surface current. Then, using the orthogonality of the modal vectors, we have

$$V_i = -\hat{Z}_i \iint J_s \cdot e_i \, ds$$

where $1/\hat{Z}_i = Y_i^o \operatorname{ctn}[K_{iz}^o (c-h)] - Y_i^1 \operatorname{ctn}(K_{iz}^1 h)$

The admittance $\hat{Y}_i$ is the parallel connection of the admittances of the covers at z=0 and z=c transformed back to the substrate surface, z=h. Multi-layered geometries need only modify $\hat{Y}_i$.

Evaluation of the V_i requires the evaluation of surface integrals of the current distribution dotted with a mode vector. We use the 'roof-top' distribution [8]. The distribution has a triangle function dependence in the direction of current flow and a rectangle function dependence in the lateral direction. This is shown in Figure 3, where the rectangular base of the figure represents the rectangular subsection and the height above the base is proportional to the current density. Figure 4 shows how several roof top functions can be placed on overlapping subsections to provide a piecewise linear approximation to the current in the direction of current flow and a step approximation in the lateral direction.

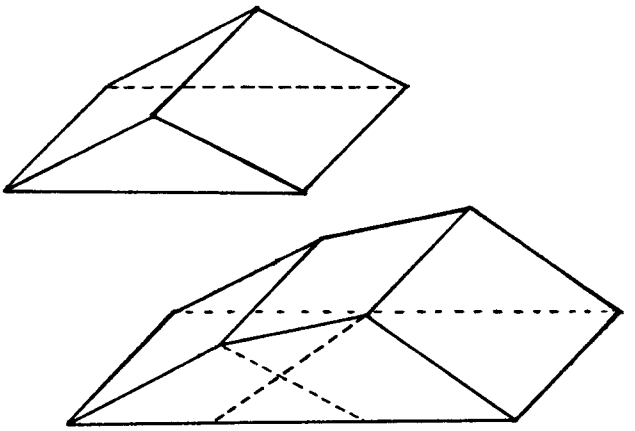

Figure 3. (top) The current density on a single subsection is a roof-top function.

Figure 4. (bottom) Two roof-top functions, end-to-end, form a piecewise linear approximation.

Initial Open Circuited Microstrip Stub Analysis

The dimensions selected for the analyses are those usually selected for "scaled" circuits. Since we have nothing from which to scale, the term scaled circuits is inappropriate. However, the reason that dimensions on the order of centimeters were chosen is the same reason that scaled circuits are used; ease of construction and measurement. Since microstrip circuits typically have dimensions on the order of $1/10^{th}$ to $1/100^{th}$ of the dimensions given here, the range of validity of this analysis for microstrip design will be 10 to 100 times the frequencies described here.

A microstrip stub 2.54 cm wide and 10 cm long contained in a box 13.0 cm long, 7.9 cm wide and 5.0 cm high was first built and measured. To ease fabrication requirements, air was used as a dielectric throughout the box.

Two measurements were made using a Hewlett Packard 8510 automated network analyzer. The first measurement was of the stub itself. Since the network analyzer was calibrated outside the box, the end of the input connector was shorted to the adjacent wall with a copper strap and measured. The connector phase length was then removed from the measurement.

The initial comparison between measured and calculated data, Figure 5, shows differences which increase with increasing frequency and at high impedance levels. The direction of the difference suggests that a shunt capacitance at the base of the stub is unaccounted for in the analysis. This shunt capacitance can be attributed to the fringing capacitance of the circular coaxial aperture formed by the input SMA connector.

A single frequency, 1.5 GHz, was selected and the required shunt capacitance calculated, 0.56 pF. This capacitance was then placed in shunt with the calculated stub input impedance at all frequencies.

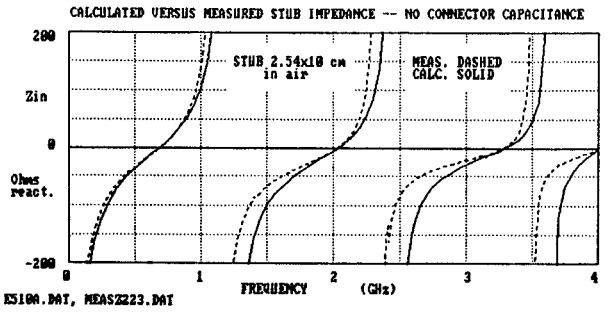

Figrue 5. Measured versus calculated prior to addition of connector capacitance.

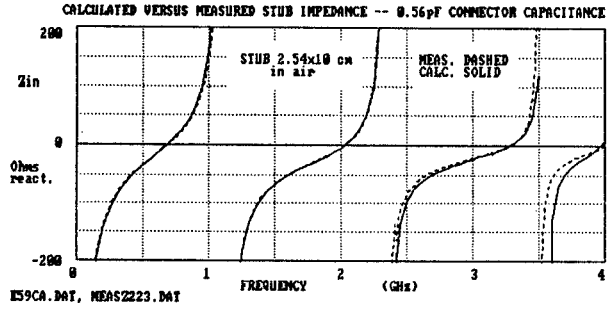

Figure 6. Substantially improved agreement when connector capacitance included.

The result is shown in Figure 6. The agreement is substantially improved, especially below 2.3 GHz.

Current on the stub was plotted at several frequencies. A distribution is shown conceptually in Figure 7. The source current is injected (by a coaxial connector) into the base of the stub. The current immediately flows to the edge of the stub. Now the current, concentrated on the edge, flows to the end, smoothly tapering to zero. Since the distribution is symmetric about the stub center line, subsequent plots show only the lower half, with the stub edge outlined.

The current distribution is indicated by a set of arrows. The length indicates the current magnitude. There is one arrow per subsection. Since a subsection will have either x or y (and not both) directed current, each arrow is either x or y directed. Since the x directed subsections are offset with respect to the y directed subsections, we find the arrows are also offset. Any arrow less than four printer dots long is left without an arrowhead. All arrows are plotted with at least one dot, no matter how small the current.

Figures 8 and 9 show current distributions at 500 MHz and 3000 MHz. At 500 MHz, we see the current injected into the center of the stub in the upper left corner of the plot. The current then proceeds down (and up, not shown due to symmetry) to the edge of the stub. Then the current propagates along the edge, smoothly tapering to zero as it reaches the end. At this frequency, the stub is a little less than $1/8^{th}$ wavelength long. The lateral current near the source is believed to be a numerical artifact of the source model.

At 3000 MHz, we see that the current at the end of the stub does not go smoothly to zero as before. This increases the electrical length of the stub and is frequently modeled as an open end fringing capacitance. Note that the current at the very end of the stub does go to zero since we use triangle functions for the current density in the direction of current flow. An additional effect is starting to appear, the lateral current at the end of the stub is growing. At higher frequencies, the current will actually wrap around the corner of the stub, further increasing electrical length.

Another interesting feature of the current distribution at this frequency is that the first current reversal on the edge of the stub is past the corner of the stub while the reversal on the interior of the stub occurs further along. The second reversal is aligned across the stub.

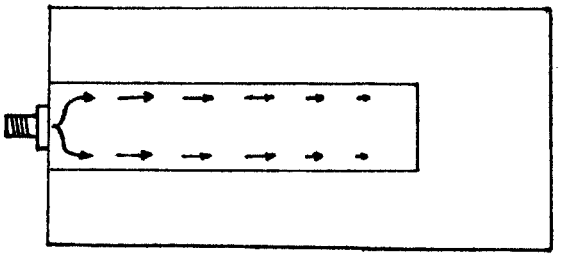

Figure 7. Conceptual illustration of current flow in microstrip stub.

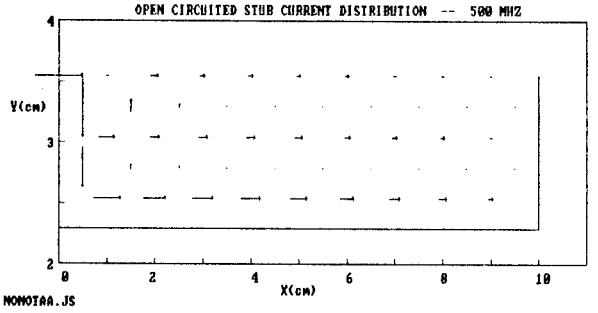

Figure 8. Stub at 1/8th wavelength long.

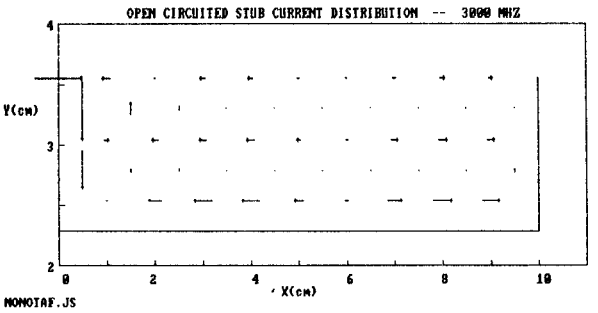

Figure 9. Stub at one wavelength long.

Notched Stub Measurement

The microstrip stub was modified by cutting a notch midway along the length of the stub. The notch was 2.0 cm long and 0.5 cm deep, changing the width of the line from 2.54 cm to 1.54 cm.

Figure 10 shows the measured versus calculated results with, now, 0.29 pF of capacitance in shunt with the calculated data. The shunt capacitance is about half of the previous case, probably due to dimensional inaccuracies in stub fabrication.

Figures 11 shows a current distribution on the notched stub. The current flows naturally around the notch. A lateral current, smaller but similar to that in the vicinity of the source, is also seen near the beginning and end of the notch.

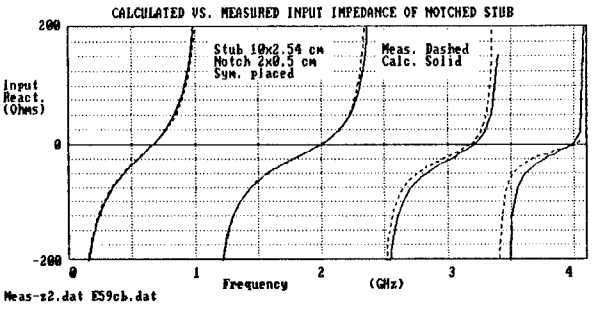

Figure 10. Measured versus calculated for notched stub.

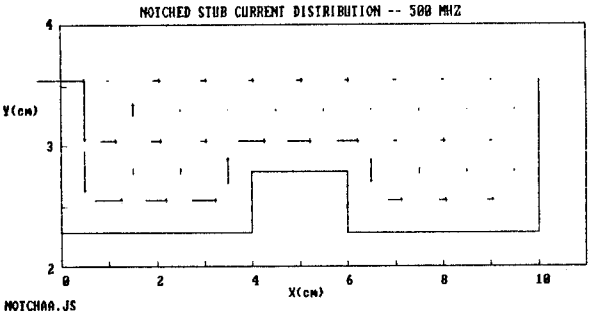

Figure 11. Current flows naturally around the notch.

CONCLUSION

We have presented a technique for the electromagnetic analysis of microstrip circuits which subdivides the microstrip metalization into rectangular subsections. The analysis was applied to several microstrip open circuited stubs with current distributions and input impedances calculated as a function of frequency. Measurements, when corrected for connector length and capacitance, agree well. All analyses in this paper were performed on an IBM-PC, illustrating the relative efficiency of the technique.

This analysis should be useful in the creation of data bases of S-parameters for specific microstrip discontinuities. As faster computers become more available, it is reasonable to consider entire microstrip circuits. The software was vectorized, so that on a parallel processing computer, analysis of circuits of several thousand subsections becomes a possibility.

ACKNOWLEDGEMENTS

This work was supported in part by an industrially supported fellowship from General Electric Company, Electronics Laboratory, Syracuse, NY 13221, and in part by the Office of Naval Research, Arlington, VA 22217 under contract Number N00014-85-K-0082.

REFERENCES

[1] R. F. Harrington, **Time-Harmonic Electromagnetic Fields**. New York: McGraw-Hill, 1961.

[2] R. H. Jansen, "The spectral-domain approach for microwave integrated circuits," **IEEE Trans. Microwave Theory.**, vol. MTT-33, pp. 1043-1056, 1985.

[3] J. C. Rautio and R. F. Harrington, "Preliminary results of a time-harmonic electromagnetic analysis of shielded microstrip circuits," **27th Automatic RF Techniques Group Conference Digest**, Baltimore, pp. 121-134, June 1986.

[4] J. C. Rautio, "A time-harmonic electromagnetic analysis of shielded microstrip circuits," Ph.D. dissertation, Syracuse University, Syracuse, NY, 1986.

[5] J. C. Rautio and R. F. Harrington, "An electromagnetic time-harmonic analysis of shielded microstrip circuits," to be published.

[6] J. C. Rautio and R. F. Harrington, "Results of an electromagnetic time-harmonic analysis of shielded microstrip circuits," to be published.

[7] J. C. Rautio and R. F. Harrington, "Efficient evaluation of the system matrix in an electromagnetic analysis of shielded microstrip circuits," to be published.

[8] A. W. Glisson and D. R. Wilton, "Simple and efficient numerical methods for problems of electromagnetic radiation and scattering from surfaces." **IEEE Trans. Antennas Propagat.**, vol. AP-28, pp. 593-603, 1980.